Analysis of Viscous-Inviscid Interaction in Transonic Internal Flows

Meng-Sing Liou*
McDonnell Douglas Corporation, St. Louis, Missouri

A method is presented to compute steady transonic flows in two-dimensional and annular diffusers, including the effects of shock/turbulent boundary-layer interaction and mass transfer through permeable walls. The analysis is based on the technique of matched asymptotic expansions and results in a system of coupled equations that describes the inviscid and turbulent boundary-layer flows. The derivation allows for the possibility of shock-induced separation in case of sufficiently strong shocks, assuming the separation bubble size is comparable to the boundary-layer thickness. The numerical procedure required to solve the system of equations is simple, and the computation times are sufficiently short to be useful in engineering design. Results are illustrated for two-dimensional and axisymmetric cases, the former showing good agreement with available experimental data.

Introduction

THIS paper describes a formal analytical theory for the computation of viscous-inviscid interactions in steady transonic flows for two-dimensional and axisymmetric diffuser configurations (Fig. 1). The flowfield under consideration is characterized by fluid acceleration from subsonic to supersonic speed, passage across a nearly normal shock, and continued subsonic deceleration in a divergent channel. Wall boundary layers are turbulent, and mass transfer (blowing or suction) through the walls is allowed. Flows of this type are present in aircraft and missile inlets, turbomachinery blade passages, wind tunnels, flowmeters, and other devices.

Steady transonic flow in nozzles has received considerable attention and theoretical treatment.[1-4] Messiter and Adamson[5] presented systematic solutions for inviscid flows with a shock in a nozzle, employing methods of matched asymptotic expansions. The same approach was used to study unsteady two-dimensional transonic flows in a channel in which the shock motion with large amplitude was allowed[6] and the boundary layers were included.[7] The region of shock wave/turbulent boundary-layer interaction was regarded as a discontinuity. In Ref. 7, linear relations of jump in displacement and momentum thicknesses with the shock strength were imposed to effectively take into account the influence of shock on the boundary layers.

Solutions described in this paper for the flowfields of Fig. 1 were constructed using the method of matched asymptotic expansions, which is valid in the dual limit of Reynolds number approaching infinity and Mach number approaching unity. By utilizing the above limits, the flowfield can be divided into several subregions (Fig. 2), each described by appropriate equations containing the terms of significant magnitude. The flowfield is split into inviscid and viscous layers in the Y direction, and into outer, inner, and shock/boundary-layer interaction regions in the X direction. Solutions valid in each region are derived and matched with those of neighboring regions, resulting in a complete representation of the flowfield.

Presented as Paper 81-0004 at the AIAA 19th Aerospace Sciences Meeting, St. Louis, Mo., Jan 12-15, 1981; submitted March 11, 1981; revision received Oct. 21, 1982.

*Research Scientist, McDonnell Douglas Research Laboratories; at present: Professor and Head, Dept. of Aeronautical Engineering, National Cheng Kung University, Tainan, Taiwan. Member AIAA.

Analysis

Using overbars to denote dimensional quantities, the nondimensional orthogonal coordinates are defined as

$$X=\bar{X}/\bar{L} \tag{1a}$$

and

$$Y=\bar{Y}/\bar{L} \tag{1b}$$

where the X axis is aligned with the direction of incoming flow, the Y axis is aligned with the minimum cross section, and $\bar{L}$ is chosen to be the throat height for all two-dimensional nonsymmetric diffusers and the half throat height for a two-dimensional symmetric or an axisymmetric diffuser. The streamwise variation of the cross-sectional area is assumed to be small such that the flow acceleration is small and the flow remains transonic. The contours of upper (outer) and lower (inner) walls, denoted by subscripts *1* and *0*, respectively, are specified in the following form:

$$Y_{w1}=1+\epsilon^2 f_1(X) \tag{2a}$$

and

$$Y_{w0}=mR+\epsilon^2 f_0(X) \qquad R<1 \tag{2b}$$

where the small parameter ϵ^2 is chosen as the nondimensional curvature of the upper (outer) wall at $X=0$. The index m defines the geometry: $m=0$ corresponds to two-dimensional flows and $m=1$ to axisymmetrix flows. R is the radius of the centerbody at $X=0$. The nondimensional turbulent boundary-layer thickness δ is assumed small on both walls, so that an inviscid core flow exists throughout the channel. The gas is assumed to follow the perfect gas law and to have constant specific heats.

The inviscid flow is assumed initially uniform, and its critical conditions, denoted by superscript *, are used as reference quantities. The nondimensional variables can be expanded in the following forms:

$$U=\bar{U}/\bar{a}^*=1+\epsilon u_1(X,Y)+\epsilon^2 u_2(X,Y)+\ldots \tag{3a}$$

$$V=\bar{V}/\bar{a}^*=\epsilon^2 v_1(X,Y)+\epsilon^3 v_2(X,Y)+\ldots \tag{3b}$$

and

$$P=\bar{P}/\bar{P}^*=1+\epsilon p_1(X,Y)+\epsilon^2 p_2(X,Y)+\ldots \tag{3c}$$

for $X=0(1)$ and $Y=0(1)$. In Eq. (3b) the transverse velocity component is caused by the area change of the diffuser and is

therefore $0(\epsilon^2)$. Expansions similar to Eq. (3c) are used for density, temperature, and stagnation enthalpy.

The first-order governing equations are found to be

$$\vec{q}\cdot\text{grad}\frac{|q|^2}{2}-a^2\text{div}\vec{q}=0 \tag{4a}$$

$$\rho U\frac{\partial}{\partial X}\vec{q}=-\frac{1}{\gamma}\text{grad}P \tag{4b}$$

$$\Delta h_t=0 \tag{4c}$$

and

$$\Delta S=0 \tag{4d}$$

where $\vec{q}=U\vec{i}+V\vec{j}$. Since no viscous terms are contained in Eqs. (4), the region where $X=0(1)$ and $Y=0(1)$ is referred to as the inviscid layer, and the solutions of Eqs. (4) are termed inviscid solutions. Appropriate boundary conditions for solving this set of inviscid equations must be imposed. In Ref. 7, the boundary conditions on the vertical velocity component as $Y\to 0$ and $Y\to 1$ were intuitively (but correctly) taken as tangency conditions at the walls that were modified by the displacement thicknesses. In the present work, a rigorous procedure is used to obtain the correct boundary conditions for the more general case of mass transfer through the walls. The resulting equations are given below. The first-order approximation is

$$u_1=u_1(X) \tag{5a}$$

$$(\gamma+1)u_1\frac{du_1}{dX}-\frac{1}{Y^m}\frac{\partial}{\partial Y}(Y^m v_1)=0 \tag{5b}$$

and the second approximation obeys

$$(\gamma+1)\frac{\partial}{\partial X}(u_1u_2)-\frac{1}{Y^m}\frac{\partial}{\partial Y}(Y^m v_2)+(\gamma-\tfrac{1}{2})u_1^2\frac{du_1}{dX}=0 \tag{5c}$$

$$\frac{\partial u_2}{\partial Y}=\frac{\partial v_1}{\partial X} \tag{5d}$$

Integration of Eq. (5b) yields

$$\frac{\gamma+1}{m+1}[1-(mR)^{m+1}]u_1\frac{du_1}{dX}=v_1(X,Y\to 1)-(mR)^m v_1(X,Y\to mR) \tag{6}$$

Since viscous boundary layers are taken into consideration, the inviscid tangency conditions, in general, cannot be used for v_1 as Y approaches the walls. The correct matching conditions for v_1 as $Y\to 1$ or $Y\to mR$ are those resulting from the boundary-layer solutions as $(Y_{w1}-Y)/\delta_1\to\infty$ or $(Y-Y_{w0})/\delta_0\to\infty$, respectively ($\delta$ is the boundary-layer thickness). These matching conditions can be obtained by integrating the continuity equation with respect to Y from Y_{w0} to Y_{w1}:

$$\frac{d}{dX}\int_{Y_{w0(X)}}^{Y_{w1(X)}}Y^m\rho U\,dY=[-Y_{w1}^m(\rho V)_{w1}+Y_{w0}^m(\rho V)_{w0}]+\left[-(\rho U)_{w1}Y_{w1}^m\frac{dY_{w1}}{dX}+(\rho U)_{w0}Y_{w0}^m\frac{dY_{w0}}{dX}\right] \tag{7}$$

where the terms in the first bracket represent the vertical component of mass transfer through the walls and the terms in the second bracket (resulting from the interchange of the order of differentiation and integration) represent the horizontal component. The latter component becomes zero for the no-slip condition, which corresponds to applying vertical blowing or suction only.

Next, the integral of Eq. (7) will be expressed in terms of boundary-layer displacement thicknesses. Since the inviscid solutions depend on Y[see Eq. (5d)], modified definitions of the displacement thicknesses are introduced:

$$\delta_1^*=\int_{Y_{1/2}}^{Y_{w1}}\left(\frac{Y}{Y_{w1}}\right)^m\left[1-\frac{\rho U}{(\rho U)_{iv}}\right]dY \tag{8a}$$

and

$$\delta_0^*=\int_{Y_{w0}}^{Y_{1/2}}\left(\frac{Y}{Y_{w0}}\right)^m\left[1-\frac{\rho U}{(\rho U)_{iv}}\right]dY \tag{8b}$$

where $Y_{1/2}\equiv(Y_{w0}+Y_{w1})/2$ and $(\rho U)_{iv}$ is the inviscid mass flow rate per unit area as determined from the solutions of Eqs. (5) and (6). Substituting Eqs. (8) in Eq. (7), and retaining the order of approximations results in

$$\frac{\gamma+1}{m+1}[1-(mR)^{m+1}]u_1\frac{dU_1}{dX}=\frac{d}{dX}[f_1-(mR)^m f_0]+\frac{1}{\epsilon^2}\frac{d}{dX}[-\delta_1^*-(mR)^m\delta_0^*]+\frac{1}{\epsilon^2}[(\rho V)_{w1}-(mR)^m(\rho V)_{w0}] \tag{9a}$$

and

$$(\gamma+1)\frac{d}{dX}\int_{mR}^{1}Y^m\left[-u_1u_2+\frac{3-2\gamma}{6}u_1^3\right]dY=0 \tag{9b}$$

The horizontal components of mass transfer are ignored in Eq. (9a) without loss of generality. Comparison of Eqs. (6) and (9a) gives the matching conditons for v_1:

$$v_1(X,Y\to 1)=\frac{df_1}{dX}-\frac{1}{\epsilon^2}\frac{d\delta_1^*}{dX}+\frac{1}{\epsilon^2}(\rho V)_{w1} \tag{10a}$$

and

$$v_1(X,Y\to mR)=\frac{df_0}{dX}+\frac{1}{\epsilon^2}\frac{d\delta_0^*}{dX}+\frac{1}{\epsilon^2}(\rho V)_{w0} \tag{10b}$$

Equations (10) represent a generalized tangency condition that properly takes into account the boundary-layer displacement and mass transfer effects. If both of these are neglected, Eqs. (10) reduce to the conventional tangency condition for inviscid flows.

Depending upon the relative order of magnitudes of δ^* and V_w compared to ϵ^2, some terms in Eqs. (10) may be negligible. Define

$$\tilde{\delta}_1^*=\frac{\delta_1^*}{\epsilon^2}\qquad\tilde{\delta}_0^*=\frac{\delta_0^*}{\epsilon^2} \tag{11a}$$

$$\tilde{M}=-\frac{1}{\epsilon^2}\frac{(\rho V)_{w1}}{(\rho U)_{iv}}\qquad\tilde{M}=\frac{1}{\epsilon^2}\frac{(\rho V)_{w0}}{(\rho U)_{iv}} \tag{11b}$$

The negative sign in Eq. (11b) ensures that blowing corresponds to positive values and that suction corresponds to negative values of $\tilde{M}$. In the following three limiting cases, only the displacement thickness $\tilde{\delta}^*$ will be involved; a similar argument can be applied for $\tilde{M}$:

1) When $\tilde{\delta}^*\gg 1$, the boundary layers are relatively thick and occupy the entire region; the inviscid layer no longer exists.

2) When $\tilde{\delta}^*=0(1)$, the effects of boundary layer and wall geometry on the flow acceleration (deceleration) are of equal importance; the inviscid and boundary-layer equations are coupled.

3) When $\tilde{\delta}^* \ll 1$, the boundary-layer modification on the inviscid solutions is formally small in a major part of the channel. However, this condition also implies that, for fixed X and $\tilde{\delta}^*$, the flow accelerations and the local Mach number could be relatively large, which in turn suggests that shock-induced separation could occur.

The governing equations derived for $\tilde{\delta}^* = 0(1)$ contain all terms of the $\tilde{\delta} \ll 1$ case, plus additional terms, all of which go to zero in the limit $\tilde{\delta}^* \to 0$. Thus the equations derived for $\tilde{\delta}^* = 0(1)$ can be regarded as composite equations valid for both cases of $\tilde{\delta}^* = 0(1)$ and $\tilde{\delta}^* \ll 1$. The composite case $\tilde{\delta}^* = 0(1)$ and $\dot{M} = 0(1)$ was thus chosen as the subject of further analysis in the remainder of the present paper.

Once the boundary conditions for v_1 are determined, Eqs. (5) and (6) can be integrated to give an explicit expression, although $\tilde{\delta}^*$ must be solved simultaneously from a set of differential equations involving u_1:

$$u_1(X,Y) = \pm\left(\frac{2(m+1)}{(\gamma+1)}\right)\frac{1}{1-(mR)^{m+1}}\left\{f_1 - \tilde{\delta}_1^* - (mR)^m(f_0+\tilde{\delta}_0^*) - \int_{X_\infty}^{X}[\dot{\tilde{M}}_1 + (mR)^m\dot{\tilde{M}}_0]\,dX\right\} + \left(\frac{c_u}{c_d}\right)^{1/2} \tag{12a}$$

$$v_1(X,Y) = \frac{\gamma+1}{m+1}u_1\frac{du_1}{dX}\left[Y - \frac{(mR)^{m+1}}{Y^m}\right] + \left(\frac{mR}{Y}\right)^m\left[\frac{d}{dX}(f_0+\tilde{\delta}_0^*) + \dot{\tilde{M}}\right] \tag{12b}$$

and

$$u_2(X,Y) = \frac{1}{1-(mR)^2}\left[\frac{Y^2}{2} - (mR)^2\ell nY\right]\left\{\frac{d^2}{dX^2}[f_1 - \tilde{\delta}_1^* - (mR)^m(f_0+\tilde{\delta}_0^*)] - \frac{d}{dX}[\dot{\tilde{M}}_1 - (mR)^m\dot{\tilde{M}}_0]\right\} + [(1-m)Y + mR\ell nY]\left[\frac{d^2}{dX^2}(f_0+\tilde{\delta}_0^*) + \frac{d\dot{\tilde{M}}_0}{dX}\right] + G(x) \tag{12c}$$

where

$$G(x) = \frac{3-2\gamma}{6}u_1^2 - \frac{1+m}{1-(mR)^2}\frac{1}{u_1}\begin{Bmatrix} d_u \\ d_d \end{Bmatrix} - \frac{1+m}{[1-(mR)^2]^2} \times \left[\frac{1-(mR)^4}{2(3+m)} + (mR)^2\left(\frac{1-R^2}{4} + \frac{R^2}{2}\ell nR\right)\right] \times \left\{\frac{d^2}{dX^2}[f_1 - \tilde{\delta}_1^* - (mR)^m(f_0+\tilde{\delta}_0^*)] - \frac{d}{dX}[\dot{\tilde{M}}_1 - (mR)^m\dot{\tilde{M}}_0]\right\} - \left\{\frac{d^2}{dX^2}(f_0+\tilde{\delta}_0^*) + (mR)^m\frac{d\dot{\tilde{M}}_0}{dx}\right\} \times \left[\frac{1-m}{2} - \frac{2mR}{1-(mR)^2}\left(\frac{1-R^2}{4} + \frac{R^2}{2}\ell nR\right)\right] \tag{12d}$$

where in Eq. (12a) the plus sign is used for supersonic flow and the minus sign for subsonic flow; and c and d in Eqs. (12a) and (12d), respectively, are integration constants which are different for solutions upstream and downstream of the shock. The respective values are denoted by subscripts u and d, respectively, and are determined by the properties of the incoming flow and the shock relations.

Using Eqs. (12) and the shock slope equation, $\partial X_s/\partial Y = -[V]/[U]$, where [ ] denotes the jump across the shock. Since boundary-layer growth and the mass transfer are included in Eq. (12b), v_1 may not be of the equal value on both sides of the shock, contrary to inviscid results. Hence the shock shape can be expressed in expanded form as

$$X_s = X_{s0} + \epsilon X_{s1}(Y) + \ldots \tag{13}$$

where X_{s0} is a constant for a nearly normal shock and the subscript s refers to the shock. As shown in Refs. 5 and 7, the first-order approximation u_1 satisfies the shock relation (which relates c_d to c_u), but the second-order approximation u_2 does not. Therefore an additional set of solutions must be found, valid in a small region near and behind the shock, that is, for $X - X_s = 0(1)$ and $Y = 0(1)$. This region is called the inner region and the solutions are the inner solutions. In the outer region, $X = 0(1)$ and $Y = 0(1)$, the flow properties change more rapidly in the Y direction, so that the first-order approximation of the flow appears one-dimensional, i.e., a function of X only. However, the streamwise length scale is smaller than the transverse one in the inner region, and the streamwise flow acceleration may be rapid enough to require the usual steady transonic small-disturbance equation. Hence the streamwise width (Δ_i) of the inner region is found to be $\Delta_i = 0(\epsilon^{1/2}\bar{L})$, and the inner coordinates are defined as

$$X^* = (X - X_{s0})/[(\gamma+1)u_{1u}\epsilon]^{1/2} \tag{14}$$

with Y unchanged and where the subscript u indicates evaluation immediately upstream of the shock. (For a detailed discussion, see Refs. 5 and 7.) The result is that composite solutions, valid in both $X = 0(1)$, $Y = 0(1)$ and $X^* = 0(1)$, $Y = 0(1)$, can be written as

$$U = 1 + \epsilon u_1(X) + \epsilon^2[u_2(X,Y) + u_2^*(X^*,Y)] + \ldots \tag{15a}$$

and

$$V = \epsilon^2 v_1(X,Y) + \epsilon^{5/2}v_2^*(X^*,Y) + \ldots \tag{15b}$$

where u_2^* and v_2^* are obtained from the linearized transonic equation for u_1 [Eqs. (5a) and (5b)], the condition of irrotationality associated with shock relation as $X^* \to 0$, and the matching conditions are given by outer solutions. The inner solutions are given by

$$u_2^*(X^*,Y) = 2(2R_1+R_2)\sum_{n=1}^{\infty}\frac{(-1)^n}{(n\pi)^2}e^{-n\pi X^*}\cos n\pi Y \tag{16a}$$

$$v_2^*(X^*,Y) = 2(2R_1+R_2)\sum_{n=1}^{\infty}\frac{(-1)^n}{(n\pi)^2}e^{-n\pi X^*}\sin n\pi Y \tag{16b}$$

for the two-dimensional planar case and

$$u_2^*(X^*,Y) = \sum_{n=1}^{\infty}B_n e^{-\lambda_n X^*}[J_0(\lambda_n Y) - A_n Y_0(\lambda_n Y)] \tag{16c}$$

$$v_2^*(X^*,Y) = \sum_{n=1}^{\infty}B_n e^{-\lambda_n X^*}[J_1(\lambda_n Y) - A_n Y_1(\lambda_n Y)] \tag{16d}$$

for the axisymmetric case where

$$B_n = 2\int_R^1\left(R_4Y^2 + R_5R\ell nY + R_6\frac{R^2}{Y^2} + R_7\right) \times \frac{J_0(\lambda_n Y) - A_n Y_0(\lambda_n Y)}{[J_0(\lambda_n) - A_n Y_0(\lambda_n)]^2}dY \tag{16e}$$

$$A_n = J_1(\lambda_n)/Y_1(\lambda_n) \tag{16f}$$

The variables $R_1, R_2, \ldots, R_7$ are functions of geometry and displacement thicknesses and are given in the Appendix. The eigenvalues λ_n, $n = 1,2,\ldots$, are the roots of the equation in-

volving Bessel functions

$$J_l(\lambda R)\,Y_l(\lambda) - J_l(\lambda)\,Y_l(\lambda R) = 0 \tag{17}$$

The condition of zero net flux across the boundary (the Neumann condition),

$$\int_{mR}^{l} Y^m u_2^*(0, Y)\,dY = 0 \tag{18}$$

yields a relation between d_d and d_u. The inner solutions contain a so-called Zierep singularity at the shock foot, which contributes to the rapid expansion of the inviscid solution immediately behind the shock. An excellent discussion of this type of singularity in transonic nozzle flows is given in Ref. 5. The cases computed so far suggest that the strength of singularity is reduced by the inclusion of boundary-layer effects, making the postshock expansion weaker.

For $Y - Y_w = 0(\delta)$ and $X^* \geq 0(1)$, the regular boundary-layer equations hold. The coupling of the inviscid and boundary-layer equations [Eqs. (10)] requires only the displacement thicknesses from the boundary-layer equations.

Outside the shock/turbulent boundary-layer interaction region, where $\partial p/\partial Y = 0$ across the boundary layers, an integral description is applicable. Within the interaction region where $\partial p/\partial Y \neq 0$, the integral description is inadequate and an improved analysis is needed and will be described later in the paper.

Turbulent Boundary-Layer Integral Equation

Based upon the coordinates of Fig. 1 and a viscous layer of thickness $0(\delta \bar{L})$, the mass-averaged governing equations near the walls are

$$\frac{\partial}{\partial X}(\rho U Y_{wj}^m) + \frac{\partial}{\partial Z_j}(\rho V Y_{wj}^m) = 0 \tag{19a}$$

$$\rho U \frac{\partial U}{\partial X} + \rho V \frac{\partial U}{\partial Z_j} = -\frac{1}{\gamma}\frac{\partial P}{\partial X} + \frac{\partial \tau}{\partial Z_j} \tag{19b}$$

and

$$\frac{\partial P}{\partial Z_j} = 0 \tag{19c}$$

where the variable Z_j is defined as

$$Z_j = Y - j + M(j-1)R \tag{20}$$

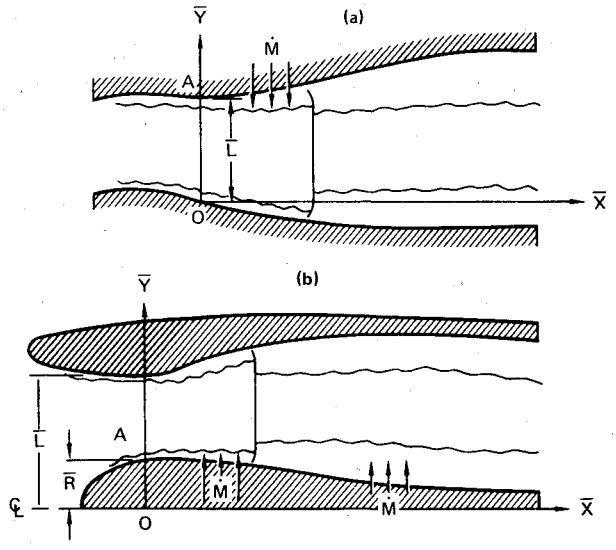

Fig. 1 Schematic of transonic internal flows: a) general two-dimensional case and b) general axisymmetric case.

where $j = 0$ or 1 for the lower- or upper-wall boundary layers, respectively, and τ is the sum of laminar and turbulent shear stresses. Since the slope of the walls is small, $0(\epsilon^2)$, the boundary-layer equations given in Eqs. (19) are identical to those written in the wall-fitted orthogonal coordinates, to the order of approximations considered in the analysis. In Eq. (19a), it is assumed that the local radius of symmetry for the axisymmetric case ($m = 1$) is larger than the boundary-layer thickness, $R \gg \delta$, which allows Y to be replaced by Y_w. Using Mager's transformation,[8] the turbulent boundary-layer equations, Eqs. (19), were transformed to an incompressible form, from which a set of integral equations was obtained by standard procedures. The resulting momentum and kinetic-energy integral equations, allowing mass transfer at the walls, are as follows (subscript j for indexing the boundary layers is omitted hereafter):

$$\frac{d\tilde{\theta}_i}{dX} + (2\tilde{\theta}_i + \delta_i^*)\frac{T_o}{T_e}\frac{1}{U_e}\frac{dU_e}{dX} = \left(\frac{T_e}{T_o}\right)^{(\gamma+1)/2(\gamma-1)}\left(\dot{M}_x + \frac{\tilde{C}_f}{2}\right) \tag{21a}$$

and

$$\frac{d\delta_i^{**}}{dX} + 3\tilde{\delta}_i^{**}\frac{T_o}{T_e}\frac{1}{U_e}\frac{dU_e}{dX} = \left(\frac{T_e}{T_o}\right)^{(\gamma+1)/2(\gamma-1)}(\dot{M}_x + \tilde{C}_D) \tag{21b}$$

where subscript i denotes variables in transformed incompressible form, subscript e refers to variables given by inviscid solutions as $Y \to Y_w$, the tilde indicates variables divided by ϵ^2, and T_o is the stagnation temperature. The skin friction coefficient C_f, the shear dissipation integral C_D, the momentum thickness θ, and the kinetic energy thickness δ^{**} are defined by

$$\tilde{C}_f = \frac{1}{\epsilon^2}\frac{2\tau_w}{\rho_e U_e^2} \tag{22a}$$

$$\tilde{C}_D = \frac{1}{\epsilon^2}\int_{z_w}^{z\to\infty}\frac{2\tau}{\rho_e U_e^2}\frac{\partial}{\partial z}\left(\frac{U}{U_e}\right)dz \tag{22b}$$

$$\theta = \frac{1}{\epsilon^2}\int_{z_w}^{z\to\infty}\delta\frac{\rho U}{\rho_e U_e}\left(1 - \frac{U}{U_e}\right)dz \tag{22c}$$

$$\delta^{**} = \frac{1}{\epsilon^2}\int_{z_w}^{z\to\infty}\delta\frac{\rho U}{\rho_e U_e}\left(1 - \frac{U^2}{U_e^2}\right)dz \tag{22d}$$

where $z = \bar{Z}/\delta$ is the boundary-layer variable. The relationships between compressible and transformed integral

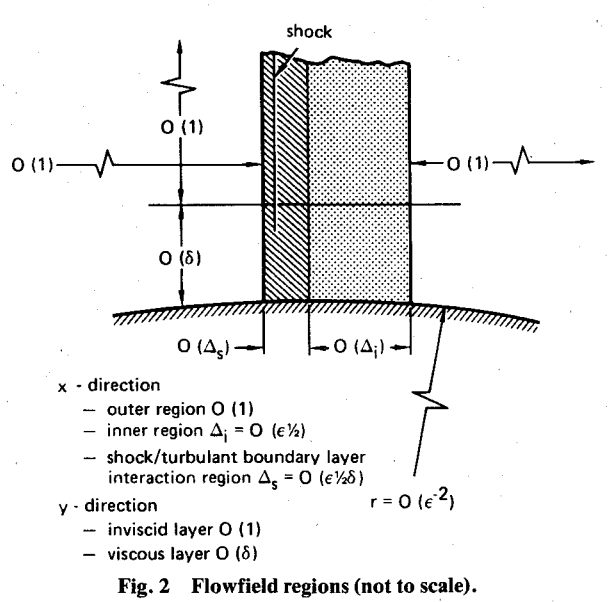

Fig. 2 Flowfield regions (not to scale).

variables are

$$\tilde{\theta} = (T_o/T_e)^{(\gamma+1)/2(\gamma-1)}\tilde{\theta}_i \tag{23a}$$

$$H = (T_o/T_e)(H_i+1) - 1 \tag{23b}$$

and

$$\tilde{\delta}^{**} = (T_0/T_e)^{(\gamma+1)/2(\gamma-1)}\tilde{\delta}_i^{**} \tag{23c}$$

Since Eqs. (21) involve five unknowns ($\tilde{\theta}_i$, $\tilde{\delta}_i^*$, $\tilde{\delta}_i^{**}$, $\tilde{C}_f$, and $\tilde{C}_D$) and only two equations, auxiliary closure relationships must be provided. Based on simplicity and demonstrated success,[9] the Ludwieg-Tillman formula[10] is chosen for $\tilde{C}_f$, and correlation models derived in Refs. 11 and 12 are used for $\tilde{C}_D$ and $\tilde{\delta}^{**}$, respectively. Even though these auxiliary correlations yield good results for impermeable walls, no guarantees can be extended to cases with mass transfer through the walls. Nevertheless, a main objective of the paper is to demonstrate explicitly the coupling of inviscid and viscous equations, and for this purpose the closure relations chosen are adequate.

Shock-Wave/Turbulent Boundary-Layer Interaction

To complete the description of the flowfield, the interaction of a shock wave and a turbulent boundary layer must be included. This interaction occurs in a rather small region, but flow properties may undergo significant changes, possibly including flow separation, which modify the character of flow downstream. An accurate prediction of the flow in the interaction region is thus required to supply the proper initial conditions for the solution of the subsonic flow downstream.

Shock/boundary-layer interactions constitute a much investigated area of research.[13-16] We employ a theoretical approach consistent with the analysis described below, namely, the method of asymptotic expansions.

Solutions are again derived under the limits as $(M_s-1)\to 0$ and $Re\to\infty$, where M_s is the Mach number just ahead of the shock and at the edge of the boundary layer. Two distinct parameters are identified as pertinent: M_s-1, representing the shock strength, and u_τ, the nondimensional friction velocity evaluated just upstream of the shock. Depending upon the relative values of u_τ and M_s-1, three different cases exist: $(M_s-1)/u_\tau \ll 1$ (Ref. 12), $(M_s-1)/u_\tau = 0(1)$ (Ref. 14), and $(M_s-1)/u_\tau \gg 1$) (Refs. 15 and 16). As this ratio increases, the shock progressively becomes stronger, and eventually flow separation can be induced.

Using the notation of this paper, M_s-1 corresponds to $U_s-1=\epsilon[u_1(X=X_s)+\epsilon u_2(X=X_s, Y=Y_w)]+\ldots$ Furthermore, the turbulent boundary layer is described asymptotically in terms of the "law of the wall" and the "law of velocity defect"[17] for a compressible flow, as was done by Maise and McDonald with considerable success.[18] Using this description, $u_\tau = 0(\delta)$ and $\delta^* = 0(u_\tau\delta)$; hence $\delta^* = 0(u_\tau^2)$, and the second and third cases correspond to the cases $\tilde{\delta}^*$ $(=\delta^*/\epsilon^2) = 0(1)$ and $\tilde{\delta}^* \ll 1$, respectively.

The streamwise extent of the interaction region Δ_s is shown to be $\Delta_s = 0[(U_s-1)^{1/2}\delta]$. Coordinates x^+ and z for the corresponding boundary layers are defined by

$$x^+ = [X - X_s(z\to 0)]/[(\gamma+1)(U_s-1)]^{1/2}\delta \tag{24a}$$

$$z = Z/\delta \tag{24b}$$

For the case of stronger shock, i.e., $U_s - 1 \gg u_\tau$, the sonic line is located close to the wall, and the shock therefore extends to the wall. A small region designated by Δ_*, which is measured by the distance between the undisturbed sonic line and the wall, is necessary to describe perturbations about the flow upstream of the shock and the initial pressure rise. However, the solution for x^+ and z held fixed describes perturbations about the flow downstream of the shock and approaches, as $x^+\to 0$ and $z\to 0$, the inner solution of $\tilde{x}\to\infty$ and $\tilde{z}\to\infty$, where $\tilde{x}$ and $\tilde{z}$ are defined later in Eqs. (27). The asymptotic structure of the interaction region is illustrated in Fig. 3. Since $\Delta_i \gg \Delta_*$ in the limit $u_\tau\to 0$, the interaction appears to occur over a flat plate. The effect of a shock on a curved wall, manifested by the Zierep singularity, was included in the solutions derived previously. The solution obtained for the shock-wave/turbulent boundary-layer interaction region can be regarded as a correction to an inviscid solution, which permits transverse pressure variation to first approximation.

Using the subscript SBLI to designate terms contributed by the interaction of the shock wave and turbulent boundary layers, the solution can be expanded as[15-16]

$$\Delta U_{\mathrm{SBLI}}(x^+, z) = u_\tau u_1^+ + u_\tau\epsilon_s u_{11} + u_\tau^2 u_2^+ + \ldots \tag{25}$$

where $\epsilon_s = U_s - 1 = U(X=X_s, Y=Y_w) - 1$. Similar expansions can be made for the other variables. Each perturbation component in Eq. (25) is the result of contributions from distributed sources along the shock, which are related to the rotationality of the boundary-layer profile. The effect of boundary-layer thickening constitutes additional corrections to u_2^+. This effect has been described as a ring source at the shock for axisymmetric pipe flow,[15,19] and is extended in the present analysis to the two-dimensional channel with two boundary layers. Thus the thickening of a boundary layer on one wall leads to a correction of order u_τ^2 to the SBLI solution associated with the other wall. As shown in Refs. 15 and 19, this shock-induced boundary-layer displacement effect is numerically significant, which implies that the effect of sidewall boundary layers may not be negligible in low aspect-ratio wind tunnel tests.

A composite solution can now be constructed by properly combining results valid in the appropriate subregions. The solution is expressed in the form

$$U = U_0(X, Y) + \Delta U_{\mathrm{SBLI}}(x^+, z) \tag{26a}$$

$$V = V_0(X, Y) + \Delta V_{\mathrm{SBLI}}(x^+, z) \tag{26b}$$

$$P = P_0(X, Y) + \Delta P_{\mathrm{SBLI}}(x^+, z) \tag{26c}$$

etc., where the subscript 0 indicates solutions described previously, i.e., Eqs. (15).

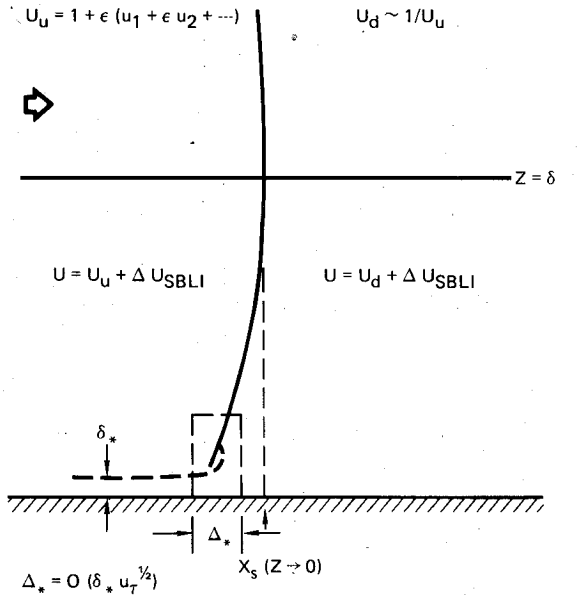

Fig. 3 Asymptotic structure of the region of interaction between a shock wave and a turbulent boundary layer (not to scale); δ_* is the incoming sonic line location, Δ_* is the thickness of the inner shock/boundary-layer interaction region.

The range of parameters chosen is such that the flow is either close to imminent separation or is separated, with a separation bubble whose length is comparable to several boundary-layer thicknesses, i.e., $U_s - 1 \gg u_\tau$. As shown in Refs. 15 and 16 (see also Fig. 3), an inner SBLI region is required for a uniformly valid description of the interaction. If the sonic line location, $\delta_* \sim \delta \exp\{-\kappa\epsilon_s[1-(\gamma-1)\epsilon_s/4+\ldots]/u_\tau - 2\Pi\kappa\}$, where the κ and Π are chosen to be 0.41 and 0.5, respectively, then the coordinates $\tilde{x}$ and $\tilde{z}$ are given by

$$\tilde{x} = [X - X_s(z/\delta \to 0)]/[(\gamma+1)u_\tau]^{1/2}\delta_* \tag{27a}$$

and

$$\tilde{z} = Z/\delta_* \tag{27b}$$

As $x^+ \to 0$ and $z \to 0$, the solution, u_1^+, in Eq. (25), should become

$$u_\tau u_1^+ \to (U_{0u} - U_{0d}) + u_\tau \tilde{u}_1(\tilde{x},\tilde{z}) + \ldots \tag{28}$$

for $\tilde{x} \to \infty$, $\tilde{z} \to \infty$, where $\tilde{u}_1$ is governed by the transonic small-disturbance equations with prescribed vorticity and appropriate boundary conditions. Although complete solution for $\tilde{u}_1$ can be obtained only numerically, it is suggested in Ref. 15 that $\tilde{u}_1$ has an exponential behavior as $\tilde{x} \to -\infty$, and a simplified method[20] can be used for connecting the solutions for u^+ and $\tilde{u}_1$.

Results and Discussion

Computations were performed for both two-dimensional and axisymmetric cases. Figure 4a shows the surface-pressure distribution on both walls of a two-dimensional diffuser; the overall agreement with the measurements made at McDonnell Douglas Research Laboratories[21] is good. The incorporation of the solution for the shock/boundary-layer interaction substantially improved the results given in Ref. 7, where a rough approximation was made for taking into consideration the jump in boundary-layer integral thicknesses. The predicted results of shock-wave/turbulent boundary-layer interaction compare well in the vicinity of the shock for weaker shock cases (Figs. 4b and 4c). By using the stronger shock limit, i.e., $(M_s - 1)/u_\tau \gg 1$, in the analysis of shock-wave/turbulent boundary-layer interaction, a flow separation which is indicated by $\tau_w < 0$ in calculation can be predicted. While the analysis would undoubtedly not be valid in largely separated flows, it may still be applicable for a separation bubble of small size, e.g., of the order of a boundary-layer thickness. It is noted that the simple auxiliary relations used for describing turbulent boundary layers can be replaced by improved equations, if desired.

Figure 5 illustrates the distribution of surface pressure for an axisymmetric duct without a centerbody in which the outer surface has the same contour as the two-dimensional case in Fig. 4. No comparable experimental data are available for this case. The isotach contours for both two-dimensional and axisymmetric cases with the same shock location are presented in Fig. 6. The general features are similar, but they differ noticeably immediately downstream of the shock. The singularity, manifested by a rapid expansion, appears stronger in the axisymmetric case, which is at least partially accounted for by the fact that the axisymmetric shock is also stronger because the effective area change from throat to shock is larger than it is in the two-dimensional diffuser.

Calculations were made for the two-dimensional case of Fig. 4a to illustrate the effects of mass transfer by prescribing an arbitrary, but convenient, distribution of suction and blowing on the upper wall, as shown in Fig. 7. The zone of mass transfer was contained fully in the subsonic region (if desired, mass transfer could be prescribed for the supersonic region in the same manner, but not in the SBLI region, since the solution there does not account for mass transfer). The details of the pressure distribution within the mass transfer zone depend strongly on the distribution of the mass flow $\dot{M}_1$. Downstream of the mass transfer region, pressure recovery is enhanced by suction and slightly degraded by blowing.

In summary, an analysis is performed to study a steady transonic flow with a shock wave in two-dimensional and axisymmetric ducts of arbitrary wall shapes. The interaction of inviscid and viscous solutions and the shock-wave/turbulent-boundary-layer interaction are described, and the effect of mass transfer at the walls is considered.

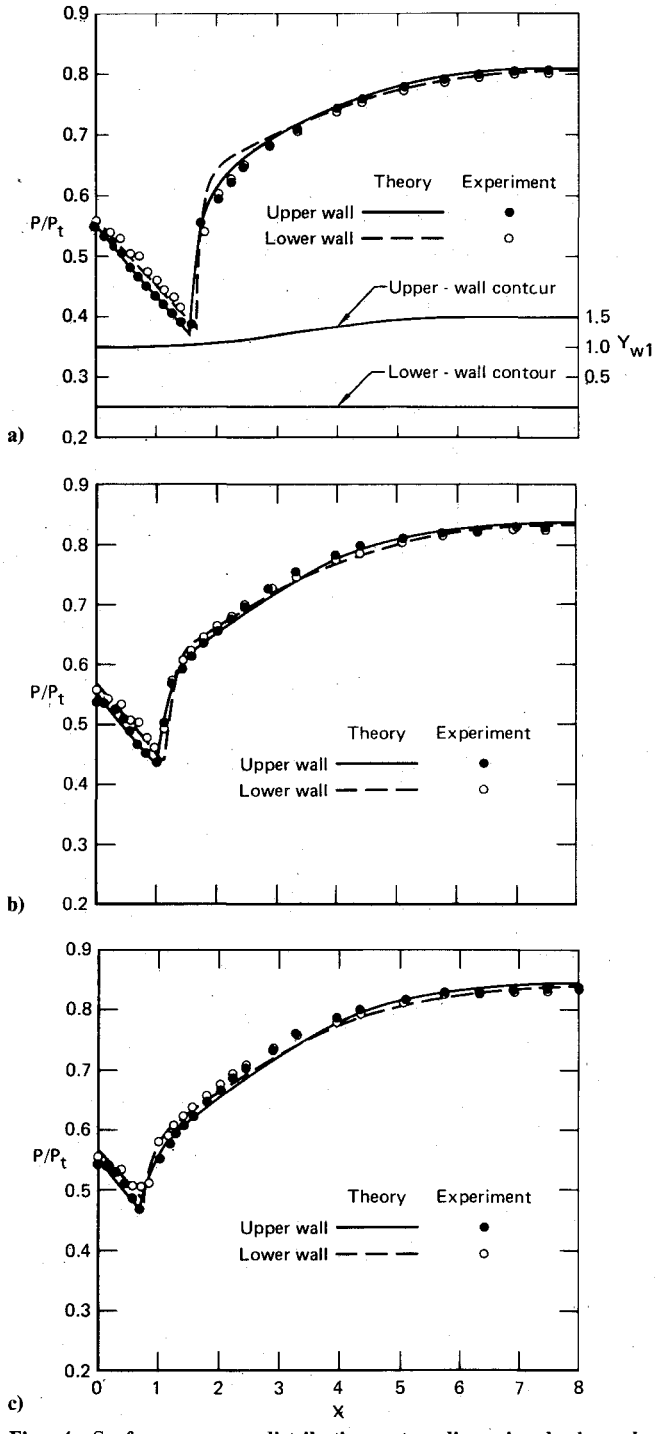

Fig. 4 Surface-pressure distributions: two-dimensional channel; initial nondimensional displacement thicknesses are 0.025 and 0.012 on the upper and lower walls, respectively, and the shape factor is 1.48 on both walls. The area ratio is 1.4 and the Mach numbers just upstream of the shock and outside of the upper-wall boundary layer are a) 1:304, b) 1:203, and c) 1:157.

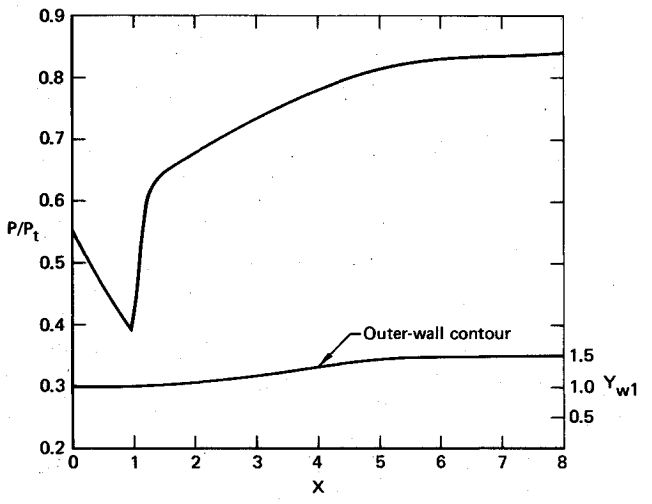

Fig. 5 Surface-pressure distribution: axisymmetric duct without a centerbody; the dimensionless displacement thickness is 0.025 and the shape factor is 1.48. Exit/throat radius ratio is 1.5 and the Mach number just upstream of the shock and outside of outer-wall boundary layer is 1.28.

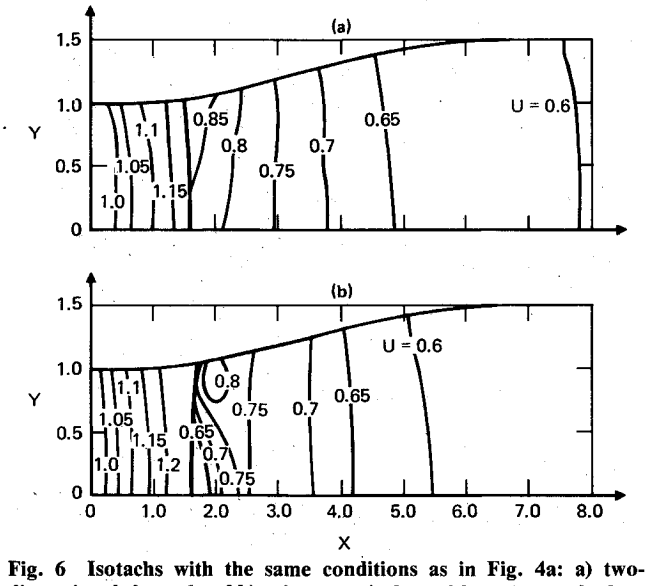

Fig. 6 Isotachs with the same conditions as in Fig. 4a: a) two-dimensional channel and b) axisymmetric duct without a centerbody.

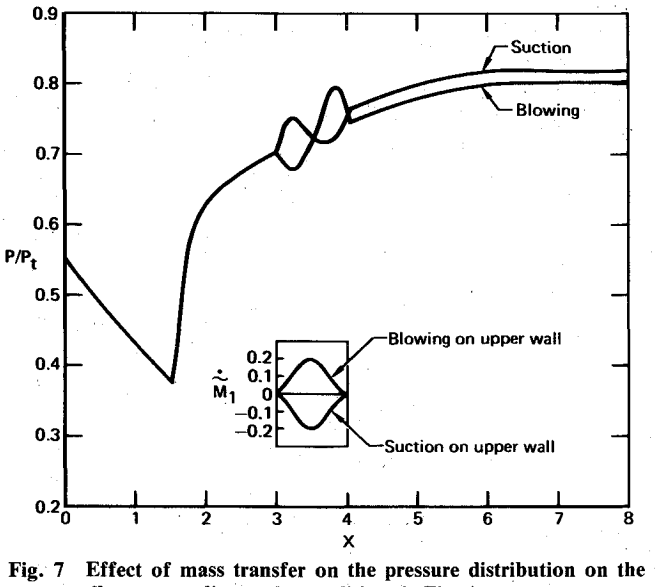

Fig. 7 Effect of mass transfer on the pressure distribution on the upper wall corresponding to the conditions in Fig. 4a.

Appendix

Detailed expressions for the variables $R_1, R_2, \ldots, R_7$ used in Eqs. (16) and (17) are

$$R_1 = -\tfrac{1}{2}\left[(G_{1X}-G_{0X})_u + (G_{1X}-G_{0X})_d\right] + \left[2/(\gamma+1)\right]Q_1^2 \tag{A1}$$

$$R_2 = -(G_{0Xu}+G_{0Xd}) + \frac{2}{\gamma+1}\frac{G_{0d}-G_{0u}}{u_{1u}}Q_1 \tag{A2}$$

$$R_3 = -(G_u+G_d) + u_{1u}^2 + \left[2/(\gamma+1)\right]Q_1^2 \tag{A3}$$

$$R_4 = -\frac{1}{2}\frac{1}{1-R^2}\left[(G_{1X}-RG_{0X})_u + (G_{1X}-RG_{0X})_d\right] + \frac{1}{(1-R^2)^2}\frac{1}{\gamma+1}Q_1^2 \tag{A4}$$

$$R_5 = -(G_{0Xu}+G_{0Xd}) + \left[1/(1-R^2)\right]\left[(G_{1X}-RG_{0X})_u + (G_{1X}-RG_{0X})_d\right] \tag{A5}$$

$$R_6 = \frac{2}{\gamma+1}\left(\frac{G_{0d}-G_{0u}}{2u_{1u}} - \frac{R}{1-R^2}Q_1\right)^2 \tag{A6}$$

and

$$R_7 = u_{1u}^2 - (G_u-G_d) + \frac{2}{\gamma+1}\frac{2}{1-R^2}Q_1\left(R\frac{G_{0d}-G_{0u}}{2u_{1u}} - \frac{R^2}{1-R^2}Q_1\right) \tag{A7}$$

where Q_1 is defined by

$$Q_1 = \left[(G_1-R^mG_0)_d - (G_1-R^mG_0)_u\right]/2u_{1u} \tag{A8}$$

The integral in Eq. (18) yields the relations

$$\tfrac{1}{3}R_1 - \tfrac{1}{2}R_2 + R_3 = 0 \tag{A9}$$

for the two-dimensional case, and

$$\tfrac{1}{4}R_4(1-R^4) - R_5R\left[\tfrac{1}{2}R^2\ln R + (1-R^2)/4\right] - R_6R^2\ln R + (R_7/2)(1-R^2) = 0 \tag{A10}$$

for the axisymmetric case. If no centerbody is included, Eq. (A10) further simplifies to

$$R_4 + 2R_7 = 0 \tag{A11}$$

Acknowledgments

This research was conducted under the McDonnell Douglas Independent Research and Development Program. The author wishes to express his appreciation to one of the reviewers, who provided many informative suggestions.

References

[1] Guderley, K. G., *The Theory of Transonic Flow,* Addison-Wesley, Reading, Mass., 1962.

[2] Ferrari, C. and Tricomi, F. G., *Transonic Aerodynamics,* Academic Press, New York, 1968, pp. 180-214.

[3] Sichel, M., "Two-Dimensional Shock Structure in Transonic and Hypersonic Flow," *Advances in Applied Mechanics,* Vol. 11, edited by C.-S. Yih, Academic Press, New York, 1971, pp. 131-207.

[4] Szaniawski, A., "Transonic Approximations to the Flow Through a Nozzle," *Archiwum Mechaniki Stosowanej,* Vol. 17, No. 1, 1965, pp. 79-85.

[5] Messiter, A. F. and Adamson, T. C. Jr., "On the Flow Near a Weak Shock Wave Downstream of a Nozzle Throat," *Journal of Fluid Mechanics,* Vol. 69, May 1975, pp. 97-108.

[6] Adamson, T. C. Jr., Messiter, A. F., and Liou, M.-S., "Large Amplitude Shock-Wave Motion in Two-Dimensional Transonic Channel Flow," *AIAA Journal,* Vol. 16, Dec. 1978, pp. 1240-1247.

[7] Liou, M.-S. and Sajben, M., "Analysis of Unsteady Viscous Transonic Flow with a Shock Wave in a Two-Dimensional Channel," AIAA Paper 80-0195, Jan. 1980.

[8] Mager, A., "Transformation of the Compressible Turbulent Boundary Layer," *Journal of the Aeronautical Sciences,* Vol. 25, No. 5, 1958, pp. 305-311.

[9] Bower, W. W., "An Analytical Procedure for the Calculation of Attached and Separated Subsonic Diffuser Flows," McDonnell Douglas Corp., St. Louis, Mo., Rept. A2589, 1973.

[10] Ludwieg, H. and Tillman, W., "Investigations of the Wall Shearing-Stress in Turbulent Boundary Layers," NACA TM1285, May 1950.

[11] Escudier, M. P. and Nicoll, W. B., "A Shear-Work-Integral Method for the Calculation of Turbulent Boundary-Layer Development," *Proceedings: Computation of Turbulent Boundary Layers-1968,* AFOSR-IFP-Stanford Conference, 1969.

[12] Alber, I. E., "Similar Solutions for a Family of Separated Turbulent Boundary Layers," AIAA Paper 71-203, Jan. 1971.

[13] Adamson, T. C. Jr. and Feo, A., "Interaction Between a Shock Wave and a Turbulent Boundary Layer in Transonic Flow," *SIAM Journal on Applied Mathematics,* Vol. 29, No. 1, 1975, pp. 121-145.

[14] Melnik, R. E. and Grossman, B., "Analysis of the Interaction of a Weak Normal Shock Wave with a Turbulent Boundary Layer," AIAA Paper 74-598, 1974.

[15] Messiter, A. F., "Interaction Between a Normal Shock Wave and a Turbulent Boundary Layer at High Transonic Speeds, Part I: Pressure Distribution," *Zeitchrift fuer Angewandte Mathematik und Physik,* Vol. 31, No. 2, 1980, pp. 204-226.

[16] Liou, M.-S. and Adamson, T. C. Jr., "Interaction Between a Normal Shock and a Turbulent Boundary Layer at High Transonic Speeds, Part II: Wall Shear Stress," *Zeitchrift fuer Angewandte Mathematik und Physik,* Vol. 31, No. 2, 1980, pp. 227-246.

[17] Coles, D. E., "The Law of the Wake in the Turbulent Boundary Layer," *Journal of Fluid Mechanics,* Vol. 1, July 1956, pp. 191-226.

[18] Maise, G. and McDonald, H., "Mixing Length and Kinematic Eddy Viscosity in a Compressible Boundary Layer," *AIAA Journal,* Vol. 6, Jan. 1968, pp. 73-80.

[19] Melnik, R. E. and Grossman, B., "Further Developments in an Analysis of the Interactions of a Weak Normal Shock Wave with a Turbulent Boundary Layer," *Symposium Transsonicum II,* edited by K. Oswatitsch and D. Rues, Springer-Verlag, Berlin, 1975, pp. 244-251; see also Grumman Research Department, Grumman Corporation, Bethpage, N.Y., Rept. RE-511, Oct. 1975.

[20] Adamson, T. C. Jr. and Messiter, A. F., "Simple Approximations for the Asymptotic Description of the Interaction Between a Normal Shock and a Turbulent Boundary Layer at Transonic Speeds," AGARD CPP-291, 1980.

[21] Sajben, M. and Kroutil, J. C., "Unsteady Transonic Flow in a Two-Dimensional Diffuser," AFOSR-TR-78-1277, May 1978.